



# Optimization of the Prismatic Core Sandwich Panel under Buckling Load and Yield Stress Constraints using an Improved Constrained Differential Evolution Algorithm

K. Malekzadeh Fard<sup>1</sup>, A.R. Pourmoayed<sup>2</sup>

<sup>1</sup> Malek Ashtar University of Technology, Tehran, Iran, Email: kmalekzadeh@mut.ac.ir

<sup>2</sup> Department of Mechanical Engineering, Khatmol Anbia Air Defense, Tehran, Iran, Email: pourmoayed@mut.ac.ir

Received August 02 2019; Revised September 09 2019; Accepted for publication September 13 2019.

Corresponding author: K. Malekzadeh Fard (kmalekzadeh@mut.ac.ir)

© 2020 Published by Shahid Chamran University of Ahvaz

& International Research Center for Mathematics & Mechanics of Complex Systems (M&MoCS)

**Abstract.** In this study, weight optimization of the prismatic core sandwich panel under transverse and longitudinal loadings has been independently investigated. To solve the optimization problems corresponding to the mentioned loadings, a new Improved Constrained Differential Evolution (ICDE) algorithm based on the multi-objective constraint handling method is implemented. The constraints of the problems are buckling load and yield stress. By comparing the results of the ICDE with those obtained by the other evolutionary algorithms based on the penalty function method in the previous studies, it is discerned that the results of the transverse loading obtained in this study are equal to those of the previous works, but the results of the ICDE in the longitudinal loading are better.

**Keywords:** ICDE algorithm, The Prismatic core sandwich panel, Constraint optimization, Transverse loading, Longitudinal loading.

## 1. Introduction

A Sandwich structure consists of two faces which primarily resist the in-plane and lateral (bending) loads and a core to withstand the shear load and prevent wrinkling of the faces. Face members are usually thin with high strength, while the core member is relatively thick and light-weight. The member selection is basically depending on the particular application and design criteria [1]. The core member can be almost any material or architecture, but in general, cores classify into four types: (a) foam or solid core, (b) honeycomb core, (c) web core, and (d) a corrugated or truss cores [2-4].

Sandwich panels with prismatic core are widely utilized in engineering applications due to high strength and lightweight properties [5]. The blast resistance and high load-bearing properties translate into a greater emphasis on these structures [6]. In addition, the porous structure of the core member facilitates the flow of fluids so they can be used as compact heat exchangers [7, 8]. Chen and Hao [9], studied a composite SIP (i.e. Structural Insulated Panel) with EPS (i.e. Expanded Polystyrene) core sandwiched that commonly is used in the building industry by flat metal skins. They also studied the effects of various specimen configurations and impact locations on their efficiency were also inquired. Valdevit et al. [10] determined the optimum weight and geometrical parameters of the prismatic sandwich panel under longitudinal loading Using a mathematical approach. The weight optimization of the sandwich panel subjected to bending was performed by Rathbun et al. [11]. Based on the sequential quadratic programming method and analytical approach, Liaghat and Serailou optimized the weight of panels with honeycomb core [12]. Yan et al. [13] Three-point bending of sandwich beams with aluminium foam-filled corrugated cores were investigated. They also were acquired in this research analytical predictions of the bending stiffness and failure modes. Traditional methods are highly

contingent on the initial values and need the gradient information of the objective function and constraints. They might be trapped in local optimum [14]. To improve the poor transverse shear resistance of corrugated sandwich cores, Bin et al. [15] were applied a combined analytical and numerical approach to exploit the idea of filling core interstices with polymer foam. Dharmasena et al. [16] Mechanical response of metallic honeycomb sandwich panel structures to high-intensity dynamic loading were investigated. They from an air blast simulation code to determine the blast loads at the front surfaces of the test panels were used, and these as inputs to finite element calculations of the dynamic response of the sandwich structure were used.

Kabir et al. [17], hemp fabrics as reinforcements with polyester resin to form composite skins were used while short hemp fibers with polyester as a core for making composite sandwich structures. In this research also, Mechanical properties such as flexural and compressive strengths of the sandwich structures made by treated and untreated hemp fibers were investigated. Li et al. [18], Mechanical response of all-composite pyramidal lattice truss core sandwich structures were investigated. Their experimental results showed that the all-composite pyramidal lattice truss core sandwich structures had more weight-efficient than other metallic lattice truss core sandwich structures. To improve the mechanical performance of the foam core sandwich composites with a rather simpler method of core reinforcement by Yalkin et al. [19] were investigated. In this study also, sandwich composites with perforated core, stitched core, and plain core have been compared in terms of compressive, bending, shear and impact performances. Via introducing Non-uniform mass distribution (gradient) in the core, substantially, the structural performance of a fully-clamped sandwich plate with square honeycomb core is achieved for out-of-plane uniform pressure loading by Yu et al. [20] were improved. Mechanical properties and failure behavior of the sandwich structures with carbon fiber-reinforced X-type lattice truss core by Wang et al. [21] were studied. Their results showed that the shear equivalent stiffness of the X-type lattice structure is independent of the loading direction, while the shear strength is related to the loading direction. Li and Wang [22], Bending behavior of sandwich composite structures with tunable 3D-printed core materials were discussed. The experimental and numerical results showed that architected core structures can be utilized to tailor the bending properties as well as failure mechanisms. In addition, the solution time can be increased significantly by increasing the number of design variables. In order to eliminate the problems mentioned above, new optimization methods have been proposed. These methods are known as the heuristic algorithms which are often inspired by nature and principles from physics. They are capable to escape from the local optimum and to find the global optimum more likely than the traditional approaches [23]. Many heuristic methods have been proposed and the number of these methods has been increased in recent years. Among them, the following algorithms can be noted: particle swarm optimization [24], harmony search [25], bat algorithm [26], firefly algorithm [27], charged system search [28], water cycle algorithm [29], dolphin echolocation [30]. Fereidoon et al. [31] used the genetic algorithm and reliability method to find the optimum weight of the sandwich panel under transverse loading. Banerjee et al. [32] used MATLAB software to determine the maximum shear strength. Hemmatian et al [33] found the optimum design of the sandwich panel under transverse loading with yielding and buckling constraints using the particle swarm optimization method; meanwhile, the imperialist competitive algorithm was used by Fereidoon et al for the same problem [34]. Mohammadian and Abolbashiari utilized the gravitational search algorithm to optimize the panel under longitudinal loading [35]. In the Multi-objective optimization of the sandwich panels, Tan and Soh optimized sandwich panels with prismatic cores to have a minimum weight and maximum heat transfer performance based on the genetic algorithm [36]. Hudson et al. proposed the application of an ant colony optimization (ACO) algorithm to the multiple objective optimization of a rail vehicle floor sandwich panel [37]. multi-objective optimization of sandwich panels using modified Non-dominated Sorting Genetic Algorithm (NSGAI) considering two objective functions, the structure's weight and deflection, was carried out by Khalkhali et al [38]. Based on the simulated annealing algorithm, Martiniez-Martin and Thrall proposed a multi-objective optimization procedure to design material properties of honeycomb core sandwich panels for minimum weight and maximum thermal resistance [39]. Another study was performed by Mohammadian and Fereidoon using multi-objective particle swarm optimization to determine optimum weight and heat transfer index of the prismatic sandwich panel [40].

In this study, weight optimization of the prismatic core sandwich panel under transverse and longitudinal loadings has been investigated independently using the Improved Constrained Differential Evolution (ICDE) algorithm based on the multi-objective constraint handling method. In section 2, the sandwich panel with the prismatic core is described and the problem statement for both transverse and longitudinal loadings is proposed. Section 3 presents the ICDE optimization algorithm. Finally, in section 4, the results are proposed and compared with those available in the literature.

## 2. Sandwich Panel with Prismatic Core

The naming of the Sandwich panels with prismatic cores is based on the number of corrugations ( $N$ ) of the core. In Fig. 1, two panels with  $N=1$  and  $N=2$ , the loading directions and the geometrical parameters are presented.  $d$ ,  $d_c$ , and  $H$  are respectively the face sheet thickness, the core member thickness, and the overall panel height. In order to maximize the transverse shear stiffness, the angle between the folded core plate and the horizontal is set to  $\theta=54.7^\circ$  [29].

## 3. Problem Statement

The goal is to find the geometric parameters  $d/l$ ,  $d_c/l$ ,  $H/l$  and  $N$  which minimize the weight of the panel per unit width. The parameter  $l$  is equal to the ratio  $M/V$  and defines a characteristic length scale related to the loading span [5].



M and V are the maximum moment and maximum shear force per unit width. The weight of the panel per unit width is given by  $W=2\rho dl+N\rho dl/\cos\theta$ , where  $\rho$  denotes the density of the material. A non-dimensional form of the weight can be re-written as

$$\Psi = \frac{W}{\rho l^2} = 2 \frac{d}{l} + \frac{N}{\cos\theta} \frac{d_c}{l} \tag{1}$$

where  $\Psi$  is the weight index.

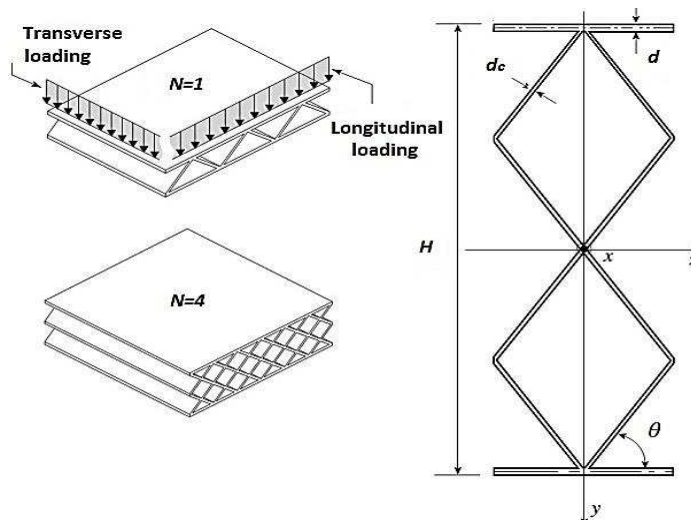


Fig. 1. Schematic of two prismatic panels: corrugated core (n=1) and diamond core (n=4) with loading directions and design parameters [10]

Eq. (1) defines the objective function of the optimization problem. The yield and buckling constraints of the problem are defined for both transverse and longitudinal loadings as follows. In the following equations,  $\Pi=V/\sqrt{EM}$  is the loading index and E is Young’s modulus of the face member and the core member.

- Constraints for the transverse loading:

$$g_1 = \Pi^2 \frac{E}{\sigma_y} \frac{l}{d} \left( \frac{H}{l} - \frac{d}{l} \right)^{-1} - 1 \quad \text{face yielding} \tag{2}$$

$$g_2 = \frac{1}{N \sin\theta} \Pi^2 \frac{E}{\sigma_y} \frac{l}{d_c} - 1 \quad \text{core yielding} \tag{3}$$

$$g_3 = \frac{48}{K_f \pi^2 N^2 \tan^2\theta} \Pi^2 \left( \frac{H}{l} - \frac{d}{l} \right) \left( \frac{l}{d} \right)^3 - 1 \quad \text{face buckling} \tag{4}$$

$$g_4 = \frac{12}{K_c \pi^2 N^3 \sin^3\theta} \Pi^2 \left( \frac{H}{l} - \frac{d}{l} \right)^2 \left( \frac{l}{d_c} \right)^3 - 1 \quad \text{core buckling} \tag{5}$$

- where  $K_f$  and  $K_c$  are defined as follows:

$$K_f = \left( \frac{2.4 \cos\theta (dc/d)^3 + 1}{1.2 \cos\theta (dc/d)^3 + 1} \right)^2 \tag{6}$$

$$K_c = 1.375 \left( \frac{2.2 + 1.2 (dc/d)^3 / \cos\theta}{1.6 + 0.6 (dc/d)^3 / \cos\theta} \right) \quad \text{if } N = 1 \tag{7}$$

$$K_c = 2.125 \quad \text{if } N \geq 2$$

where  $\sigma_y$  is yield strength.

- Constraints for the longitudinal loading:

$$G_1 = \Pi^2 \frac{E}{\sigma_y} \frac{\sqrt{N^2 + \frac{3}{\tan^2 \theta} \left( \frac{H-d}{l} \right)^2}}{\left[ N \frac{d}{l} + \frac{N^2 d_c}{6 \cos \theta l} \right] \left( \frac{H-d}{l} \right)} - 1 \quad \text{face yielding} \quad (8)$$

$$G_2 = \Pi^2 \min_{y \in \left[ 0, \frac{H-d}{2} \right]} \left\{ \frac{\frac{\sigma_y \left( \frac{H-d}{l} \right) \left[ \frac{d}{l} + \frac{N d_c}{6 \cos \theta l} \right]}{E \left( \frac{H-d}{l} \right) \left[ \frac{d}{l} + \frac{N d_c}{6 \cos \theta l} \right]}}{\sqrt{4 \left( \frac{y}{H-d} \right)^2 + 3A^2}} \right\} - 1 \quad \text{core yielding} \quad (9)$$

$$G_3 = \Pi^2 \frac{24(1-\nu^2)}{K_c \pi^2 N^2 \tan^2 \theta} \left( \frac{l}{d} \right)^2 \left( \frac{H-d}{l} \right) \left[ \frac{1}{2} \frac{l}{d} + \frac{N d_c}{12 \cos \theta l} \right]^{-1} - 1 \quad \text{face buckling} \quad (10)$$

$$G_4 = \Pi^2 \left( \Pi_{cb}^2 \right)^{-1} - 1 \quad \text{core buckling} \quad (11)$$

where

$$A = \frac{1}{n \tan \theta} \left( \frac{H-d}{l} \right) \frac{d}{l} \frac{l}{d_c} + \frac{1}{\sin \theta} \left( \frac{1}{4} - \left( \frac{y}{H-d} \right)^2 \right) \quad (12)$$

and the values of  $\Pi_{cb}^2$  (square of load index in core buckling) for different values of N are as follows:  
For  $N=1$

$$\Pi_{cb}^2 = \frac{B}{C \sqrt{\frac{1}{K_b^2} + D \left[ \frac{1}{n \tan \theta} \frac{d}{l} \frac{l}{d_c} + \frac{1}{4 \sin \theta} \right]^2}} \quad (13)$$

where

$$B = \frac{\pi^2 \sin^2 \theta}{12(1-\nu^2)} N^2 \left( \frac{d_c}{l} \right)^2 + \left( \frac{d}{l} + \frac{N d_c}{6 \cos \theta l} \right) \quad (14)$$

$$C = \frac{H-d}{l} \quad (15)$$

$$D = \frac{1}{K_s^2} \left( \frac{H-d}{l} \right)^2 \quad (16)$$

For  $N=2$

$$\Pi_{cb}^2 = \frac{B}{C \sqrt{\frac{1}{K_{cb}^2} + D \left[ \frac{1}{n \tan \theta} \frac{d}{l} \frac{l}{d_c} + \frac{1}{4 \sin \theta} \right]^2}} \quad (17)$$

For  $N \geq 4$

$$\Pi_{cb}^2 = \min \left\{ \left( \Pi_{cb}^2 \right)^{N \geq 4, inner}, \left( \Pi_{cb}^2 \right)^{N \geq 4, outer} \right\} \quad (18)$$

where

$$\left(\Pi_{cb}^2\right)^{N \geq 4, inner} = \frac{B}{C \sqrt{\frac{1}{K_{cb}^2} + D \left[ \frac{1}{n \tan \theta} \frac{d}{l} \frac{l}{d_c} + \frac{1}{4 \sin \theta} \right]^2}} \tag{19}$$

$$\left(\Pi_{cb}^2\right)^{N \geq 4, outer} = \frac{B}{C \sqrt{\frac{1}{K_{cb}^2} + D \left[ \frac{1}{n \tan \theta} \frac{d}{l} \frac{l}{d_c} \right]^2}} \tag{20}$$

where  $K_c=4$ ,  $K_s=5.35$ ,  $K_b=23.9$  and  $K_{cb}=7.81$  [10]. The optimization problems can be summarized as follows:

$$\begin{cases} \min \Psi \\ \text{s. to } g_i \leq 0 \quad i = 1, 2, 3, 4 \end{cases} \quad \text{For transverse loading} \tag{21}$$

$$\begin{cases} \min \Psi \\ \text{s. to } G_i \leq 0 \quad i = 1, 2, 3, 4 \end{cases} \quad \text{For longitudinal loading} \tag{22}$$

where  $g_i$  and  $G_i$  ( $i=1,2,3,4$ ) are respectively given by Eq. (2-7) and (8-10).

### 4. Improved Constrained Differential Evolution Algorithm

Because of the robustness and ease of implementation of the evolutionary algorithms (EAs), a lot of constrained optimization evolutionary algorithms (COEAs) have been proposed by combining the constraint-handling techniques and EAs. COEAs need to achieve two goals. The first goal is to enter the feasible region promptly, and the second goal is to find the feasible optimal solution [42]. The existing constraint handling methods can be classified into three groups: methods based on penalty functions, methods based on the preference of feasible solutions over infeasible solutions, and methods based on multi-objective optimization techniques. Penalty functions are the oldest constrained handling method. Although they are easy to use, finding an appropriate penalty function for an optimization problem, in general, requires a lot of fine-tuning. In addition, the performance of the algorithm tends to depend on it [43]. In contrast to all previous studies based on the penalty function, in this study, the ICDE algorithm based on the multi-objective constraint-handling technique is utilized to find the optimum weight of the prismatic core sandwich panel. So there is no need for the trial and error process of finding appropriate penalty parameters. The ICDE is the latest version of the differential evolution (DE) algorithm in order to solve constrained optimization problems. It includes two main parts, the Improved ( $\mu+\lambda$ )-differential evolution (IDE) to search in the design space and the archiving-based adaptive tradeoff model (ArATM) to handle the constraints of the problem. Further information and details are available at the Reference [44].

#### 4.1 Differential Evolution algorithm

The differential evolution (DE) is a population-based algorithm which is developed by Storn and Price [45] widely used to solve continuous optimization problems. An original scheme of the DE consists of four steps as:

##### Step 1: forming an initial population

After defining both upper and lower bounds of the variables, create an initial population  $P_t$  of NP individuals by randomly sampling

##### Step 2: generating the mutant vectors

Four popular mutation operations used in the DE algorithm as follows

$$rand/1: \quad \vec{v}_i = \vec{x}_{r1} + F(\vec{x}_{r2} - \vec{x}_{r3}) \tag{23}$$

$$rand/2: \quad \vec{v}_i = \vec{x}_{r1} + F(\vec{x}_{r2} - \vec{x}_{r3}) + F(\vec{x}_{r4} - \vec{x}_{r5}) \tag{24}$$

$$current - to - rand / 1: \vec{v}_i = \vec{x}_{r1} + F(\vec{x}_{r2} - \vec{x}_{r3}) + F(\vec{x}_{r4} - \vec{x}_{r5}) \tag{25}$$

$$current - to - best / 1: \vec{v}_i = \vec{x}_i + F(\vec{x}_{best} - \vec{x}_i) + F(\vec{x}_{r1} - \vec{x}_{r2}) \tag{26}$$

where  $F$  is randomly chosen between 0 and 1 and integers  $r_1, r_2, r_3, r_4, r_5$  are randomly selected such that  $r_1 \neq r_2 \neq r_3 \neq r_4 \neq r_5, x_i$ , and  $x_{best}$  are the current and best individual in the population respectively. If the boundary constraints are violated, the



components  $v_{ij}$  of mutant vectors  $v_i$  are modified as follows:

$$v_{i,j} = \begin{cases} 2L_j - v_{i,j} & \text{if } v_{i,j} < L_j \\ 2U_j - v_{i,j} & \text{if } v_{i,j} > U_j \\ v_{i,j} & \text{otherwise} \end{cases} \quad (27)$$

where  $L_j$  and  $U_j$  are respectively the lower bound and upper bound of  $j$ th variables.

**Step 3: Crossover**

Create a trial vector  $u_i$  by replacing some elements of the mutant vector  $v_i$  via the binomial crossover operation

$$u_{i,j} = \begin{cases} v_{i,j} & \text{rand} < CR \text{ or } j = j_{rand} \\ x_{i,j} & \text{otherwise} \end{cases} \quad (28)$$

where  $i \in \{1, 2, \dots, NP\}$ ,  $j \in \{1, 2, \dots, n\}$ ,  $rand$  is a uniformly distributed random number between 0 and 1,  $j_{rand}$  is an integer selected from 1 to  $n$  and  $CR$  is the crossover control parameter.

**Step 4: comparing the trial vector and the current vector**

Compare the trial vector compare with the current vector based on their objective function values and the better one will survive in the next generation

$$\vec{x}_i = \begin{cases} \vec{u}_i & \text{if } f(\vec{u}_i) < f(\vec{x}_i) \\ \vec{x}_i & \text{otherwise} \end{cases} \quad (29)$$

**4.2 Improved ( $\mu + \lambda$ ) differential evolution (IDE) algorithm**

From  $\mu$  individuals in the parent population  $P_t$ , a new offspring population  $Q_t$  with  $\lambda$  individuals is generated by utilizing the “rand/1”, the “rand/2” and the “current-to-rand/best/1” mutation strategy. The last mutation strategy is used to increase the speed of the evolvement of the last offspring to the optimal value. The formulation for the “current-to-rand/best/1” mutation strategy is proposed in the reference [44]. The IDE scheme has two main steps as follows:

**Step 1: Initialization**

Set  $Q_t = \emptyset$  and Create an initial population  $P_t$  of  $N_p$  individuals, via randomly sampling. Note that at the beginning step, the formation of the null set ( $Q_t = \emptyset$ ) is required and  $\emptyset$  is a null set.

**Step 2: generate offspring**

For each individual in  $P_t$ , generate three offspring as follows

- Generate the first offspring  $y_1$  by using the “rand/1” strategy (using Eq. (23) and (28))
- Generate the second offspring  $y_2$  by using the “rand/2” strategy (using Eq. (24) and (28))
- $Q_t = \vec{y}_1 \cup \vec{y}_2 \cup \vec{y}_3$  Generate the third offspring  $y_3$  by using the “current-to-rand/best/1” and BGA<sup>1</sup> mutation.
- Update the offspring population,

If the current generation number is greater than a threshold generation number, the last mutation strategy “current-to-rand/best/1” is performed by switching from Eq. (25) to Eq. (26).

Eq. (25) enhances the global search ability by choosing the information randomly from the search space, while Eq. (26) uses the information of the best individuals in the current population to find the global optimum. Hence, the “current-to-rand/best/1” strategy can maintain the balance between the diversity and the convergence of the population.

**4.3 Archiving-based adaptive tradeoff model (ArATM)**

Three situations exist in the combined population  $H_t = P_t + Q_t$  including the infeasible, the semi-feasible, and the feasible situations. For each of these situations, a different constraint-handling mechanism is designed in the ArATM.

**- Infeasible situation:**

In this case, all individuals violate the constraints of the problem. the original problem transformed into a bi-objective optimization problem and a good tradeoff between two objects, the objective function and the degree of constraint violation, is established. The aim of the corresponding mechanism is to guide the infeasible population toward the feasible region in the early stage of the evolution and to maintain its diversity.

<sup>1</sup> Breeder Genetic Algorithm



**- Semi-feasible situation:**

In the semi-feasible situation, both feasible and infeasible individuals exist in the combined population  $H_t$ . In this situation, some infeasible individuals who contain important information are also utilized to guide the search toward the global optimum. By implementing an adaptive fitness transformation scheme, not only some feasible individuals with small fitness values but also some infeasible individuals with both small degree of constraint violation and small fitness values survive into the next generation.

**- Feasible situation:**

Finally, in a feasible situation, all individuals in the combined population  $H_t$  are in the feasible region. The comparison between all individuals is implemented only by considering their fitness values. Therefore,  $\mu$  individuals with the smallest fitness value constitute the next population  $P_{t+1}$ . It is noted that in the above equations  $t$  is the iteration number of the optimization algorithm. The optimization process is terminated after a fixed number of iterations. The flowchart of the algorithm is shown in Fig. 2.

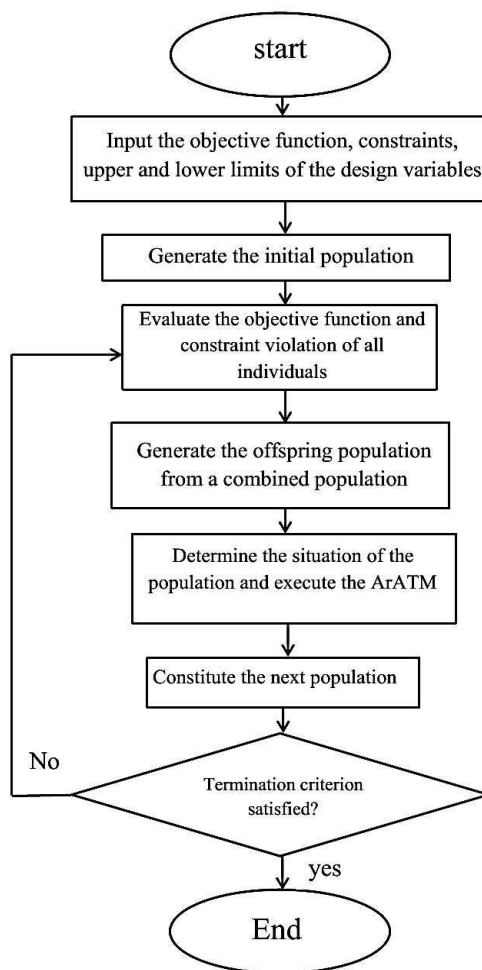


Fig. 2. Flowchart of the ICDE Algorithm

**5. Results**

In this section, at first, the results of the weight optimization of the prismatic core sandwich panel under transverse loading with yielding and buckling constraints are proposed. Next, the results corresponding to longitudinal loading is presented. The ICDE algorithm is coded in MATLAB software. The sandwich panel is made of a high strength aluminum alloy (density=2800 kg/m<sup>3</sup>, yield strength  $\sigma_y= 490 MPa$  and Young's modulus  $E=70GPa$ ). The ICDE runs 20 times independently for each optimization problem. The parameters in the ICDE algorithm are shown in Table 1. For the reach loading case, the results are compared with those available in the literature.

Table 1. ICDE algorithm's parameters for weight optimization

$\mu$	$\lambda$	F	CR
60	180	0.8	0.9

### 5.1 Sandwich panel under transverse loading

As mentioned before, the optimization problem corresponding to the transverse loading is defined by Eq. (21). The optimization task is executed for four different values of the order of corrugation ( $N=1,2,4,8$ ) and nine values for load index  $\Psi$  (from 0.0004 to 0.0022 with an increment of 0.0002). The Variation of design variables ( $H/l$ ,  $d/l$ ,  $d_c/l$ ) and weight index with respect to different transverse loading index ( $\Pi$ ) for different core corrugate numbers are shown in Figs. 3 to 6. It is assumed that the design variables are restricted to the following ranges[33]:  $0.01 < H/l < 0.2$ ,  $0.001 < d/l < 0.01$  and  $0.0001 < d_c/l < 0.003$ .

As can be seen in Figs 3 to 6, by increasing  $N$  and assuming a constant value for  $\Pi$ , the optimum values of the face sheet thickness and core member thickness increases, while the weight index decreases. So, panels with  $N=4$  and  $N=8$  are two optimum panels for the transverse loading case.

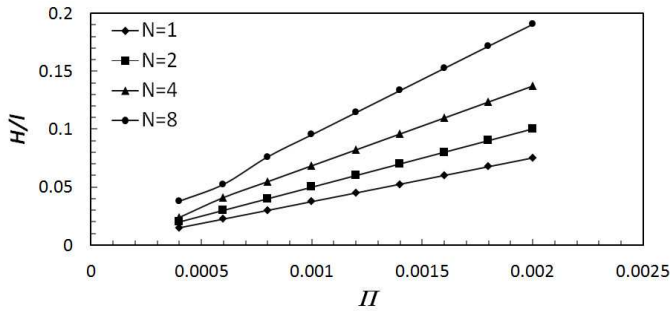


Fig. 3. Optimum normalized panel height with respect to load index in the transverse loading

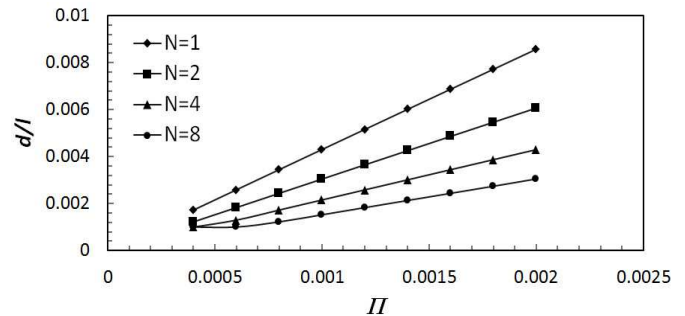


Fig. 4. Optimum normalized face thickness with respect to load index in the transverse loading

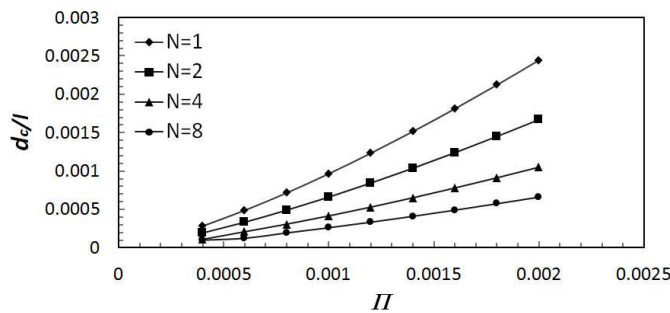


Fig. 5. Optimum normalized core member thickness with respect to load index in the transverse loading

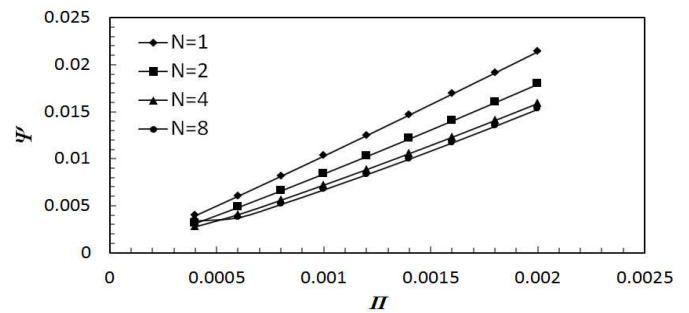


Fig. 6. Optimum weight index with respect to load index in the transverse loading

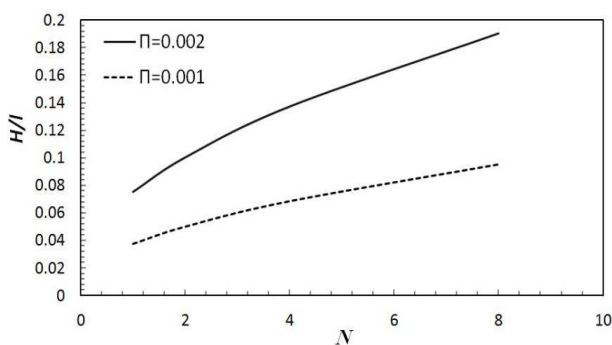


Fig. 7. Optimum normalized panel height with respect to the order of corrugation in the transverse loading

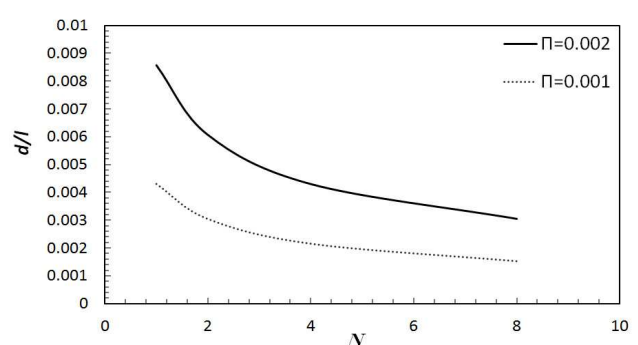


Fig. 8. Optimum normalized face thickness with respect to the order of corrugation in the transverse loading

In order to investigate the effect of the load index parameter, the variations of the design variables in terms of two load index values are plotted in Figs 7 to 10. In a constant value of  $N$ , the optimum values of  $H/l$ ,  $d/l$ ,  $d_c/l$ , and  $\Psi$  are increased by enhancing the load index. It is interesting to note, in contrast to the variables,  $d/l$ ,  $d_c/l$ , and  $\Psi$  with lowering behavior, the variable  $H/l$  has a rising behavior for both load index values. As can be observed in Figs 6 and 10, at a specific load index value, the rate of decreasing of the optimum weight index is decreased and tends to zero by increasing  $N$ . In other words, for larger values of  $N$  there is no weight reduction.

Since there is no significant weight reduction, increasing  $N$  from 4 to 8 could not be suitable for some applications due to size restrictions. So, it can be concluded that the panel with  $N=4$  is the better choice in the transverse loading. Also, the



proposed algorithm has the necessary capability for objective functions with different constraints. In the example given by the constraints, the weight function is minimized. Due to buckling constraints and yield stress, the weight is reduced slightly, which is very important in the aerospace industry and reduces fuel consumption over long flight time. Naturally, if we reduce the constraints, the weight decreases with a higher proportion.

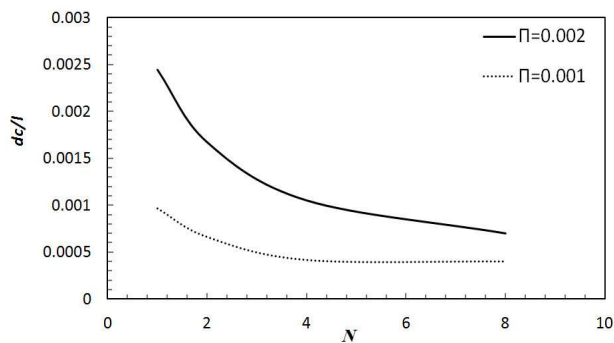


Fig. 9. Optimum normalized core member thickness with respect to the order of corrugation in the transverse loading

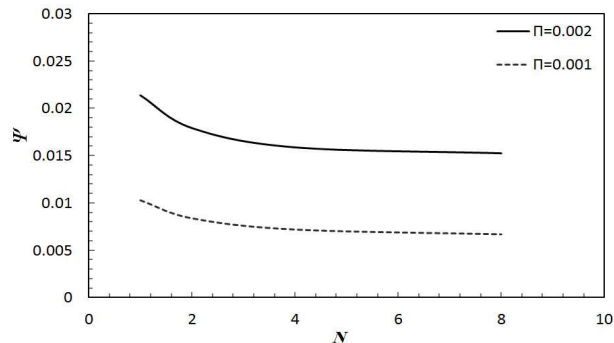


Fig. 10. Optimum weight index with respect to the order of corrugation in the transverse loading

Table 2. Optimum design variables and weight index obtained from ICDE, ICA [34] and PSO [33] algorithms in transverse loading

$\psi$	$H/l$	$d_c/l$	$d/l$	Algorithm	$\Pi$	$N$
0.0102788	0.0374979	0.0009658	0.0043037	ICA	0.001	1
0.010278	0.0375	0.000966	0.004303	PSO		
0.0102782	0.03750007	0.0009658	0.0043033	ICDE		
0.0213766	0.0752292	0.0024448	0.0085728	ICA	0.002	1
0.021376	0.075231	0.00245	0.008573	PSO		
0.0213758	0.0752306	0.0024448	0.0085725	ICDE		
0.0083783	0.0499748	0.0006617	0.0030440	ICA	0.001	2
0.008378	0.049975	0.000662	0.003044	PSO		
0.0083783	0.0499747	0.0006617	0.0030439	ICDE		
0.0179192	0.1002610	0.0016712	0.0060675	ICA	0.002	2
0.017918	0.100264	0.001671	0.006066	PSO		
0.0179175	0.1002639	0.0016714	0.0060662	ICDE		
0.0071946	0.0684310	0.0004166	0.0021555	ICA	0.001	4
0.007193	0.068456	0.000417	0.002155	PSO		
0.0071929	0.0684560	0.0004166	0.00215466	ICDE		
0.0159234	0.1356380	0.0010427	0.0043526	ICA	0.002	4
0.015875	0.137235	0.001051	0.004299	PSO		
0.0158755	0.1372347	0.0010515	0.0042985	ICDE		
0.0067049	0.0921582	0.0002565	0.0015771	ICA	0.001	8
0.006681	0.09522	0.000262	0.001525	PSO		
0.0066807	0.0952204	0.0015247	0.0015247	ICDE		
0.0152713	0.1834821	0.0006443	0.0031758	ICA	0.002	8
0.0152492	0.19041	0.000661	0.00305	PSO		
0.0152492	0.1904129	0.0030498	0.0030498	ICDE		

A comparison of the results obtained by the ICDE algorithm and those that are available in the literature are presented in Fig. 11. and Table. 2. It can be seen that the proposed methods are converged to the same weight index values corresponding to the specific values of  $N$  and  $\Pi$ .

### 5.2 Sandwich panel under longitudinal loading

The optimization problem corresponding to the longitudinal loading is given by Eq. (22) in section 2. The optimization task is performed for the same values of the order of corrugation and load index as the previous section. In Figs 12 to 15, The Variation of design variables and weight index with respect to different longitudinal loading index ( $\Pi$ ) and different core corrugate numbers are proposed. Also, the ranges of the design variables are set similar to those corresponding to the previous loading case.

The results show that, by increasing  $N$  and assuming a constant value for  $\Pi$ , in order to prevent the yielding and buckling of the sandwich panel, the optimum values of  $d/l$  and  $d_c/l$  fall, while those of  $H/l$  and  $\psi$  rise. So, panels with  $N=1$  and  $N=2$  are two optimum panels for this loading case. However, the optimum panel with  $N=1$  is an appropriate choice for applications with size restrictions.



**Table 3.** Optimum design variables and weight index obtained from ICDE, GS [35], PSO [40] and reference [10] in longitudinal loading

$\psi$	$H/l$	$d_c/l$	$d/l$	Algorithm	$\Pi$	$N$
0.007605	-	-	-	PSO	0.001	1
0.007606	0.047443	0.001022	0.002919	GS		
0.0074553	0.0486245	0.0010467	0.0028220	ICDE		
0.015216	-	-	-	PSO	0.002	2
0.015219	0.097541	0.002283	0.005634	GS		
0.0151911	0.0971525	0.0022762	0.005625	ICDE		
0.007701	-	-	-	PSO	0.001	2
0.007576	0.058648	0.001092	0.001897	GSA		
0.0074689	0.0602491	0.0011170	0.0018013	ICDE		
0.015138	-	-	-	PSO	0.002	2
0.015192	0.119464	0.002203	0.003783	GS		
0.0149688	0.1206033	0.0022431	0.0036025	ICDE		
0.008505	-	-	-	PSO	0.001	2
0.008414	0.06565	0.000857	0.001241	GS		
0.0083878	0.0691611	0.0009084	0.0010498	ICDE		
0.016854	-	-	-	PSO	0.002	4
0.016819	0.130386	0.001705	0.002508	GS		
0.0167790	0.1383867	0.0018172	0.0020999	ICDE		
-	-	-	-	PSO	0.001	8
0.008423	0.072654	0.000479	0.000892	GS		
0.0083874	0.0691844	0.0004544	0.0010482	ICDE		
-	-	-	-	PSO	0.002	8
0.016832	0.148782	0.000981	0.001623	GS		
0.0167763	0.1384011	0.0009090	0.0020956	ICDE		

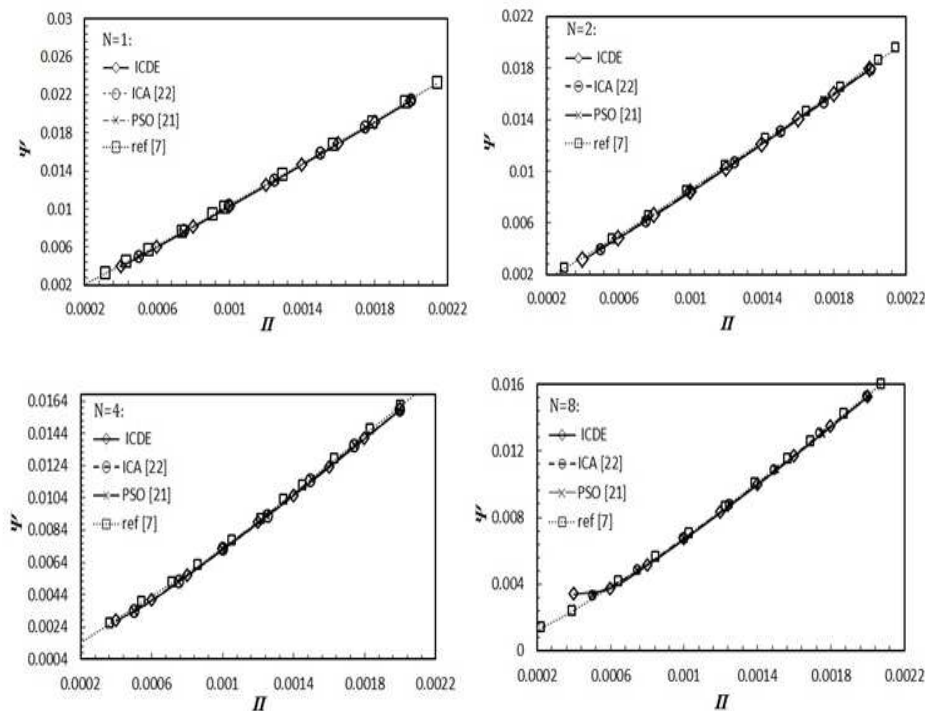


**Fig. 11.** Comparison of the results obtained by ICDE algorithm with ICA [34] and PSO [33] and reference [10] in the transverse loading

Figs 16 to 19 show the effect of the load index on the optimum design parameters. At a specific value of  $N$ , the optimum values of  $H/l$ ,  $d/l$ ,  $d_c/l$  and  $\psi$  rise as the load index is increased. In contrast to the other variables,  $H/l$  and  $\psi$  has a rising behavior for both load index values. From Fig. 19, the growing rate of the optimum weight index is negligible for  $N > 4$ .

Fig. 20 and Table 3 demonstrate the Comparison of the results obtained by the ICDE algorithm and those in the previous. As one can be seen, for all values of  $N$  and  $\Pi$ , the ICDE algorithm shows better results compared to the other methods.



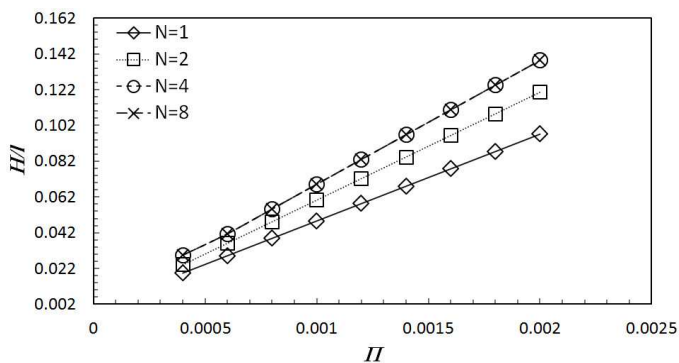


Fig. 12. Optimum normalized panel height with respect to load index in the longitudinal loading

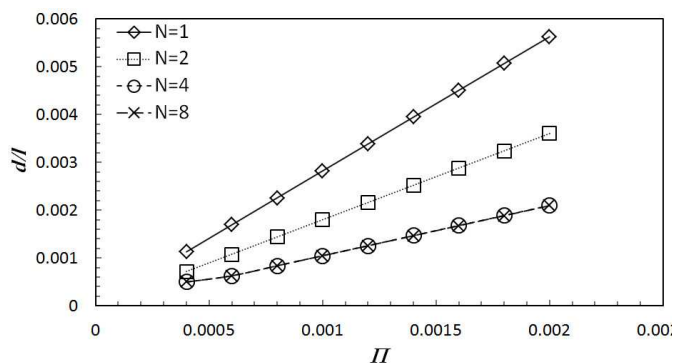


Fig. 13. Optimum normalized face thickness with respect to load index in the longitudinal loading

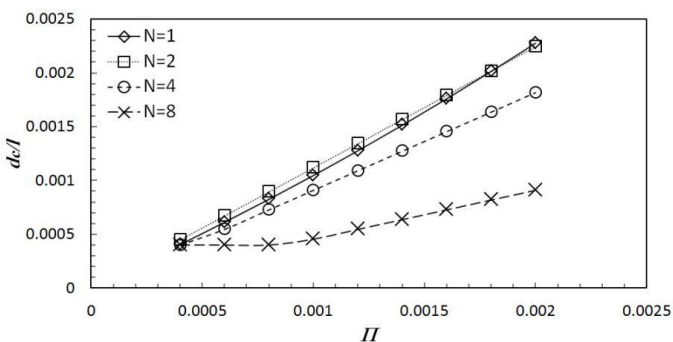


Fig. 14. Optimum normalized core member thickness with respect to load index in the longitudinal loading

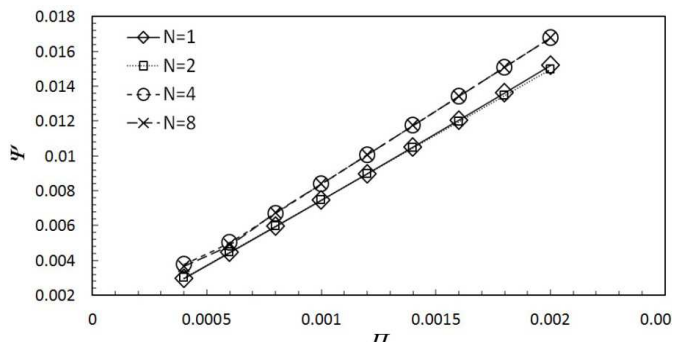


Fig. 15. Optimum weight index with respect to load index in the longitudinal loading  $H/l$

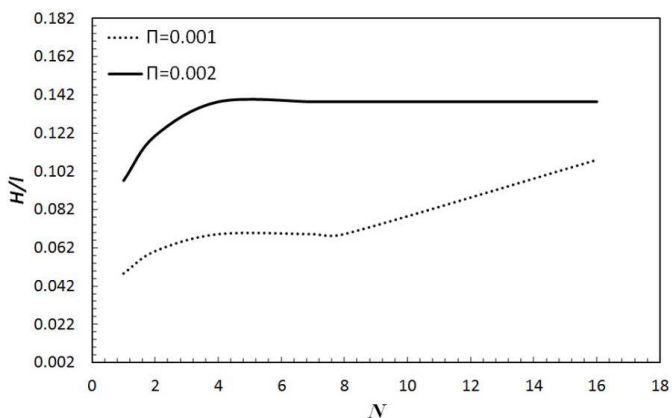


Fig. 16. Optimum normalized panel height with respect to the order of corrugation in the longitudinal loading

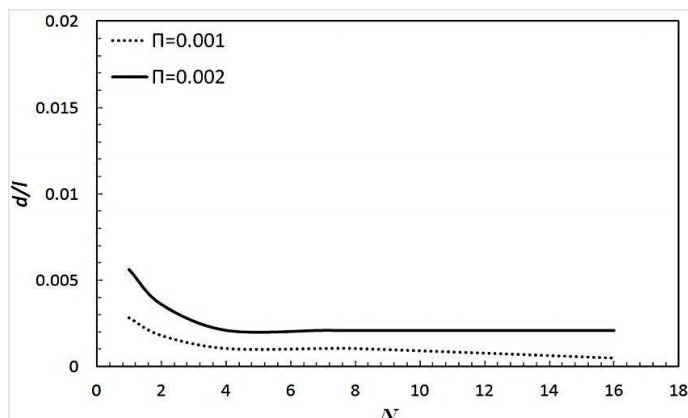


Fig. 17. Optimum normalized face thickness with respect to the order of corrugation in the longitudinal loading

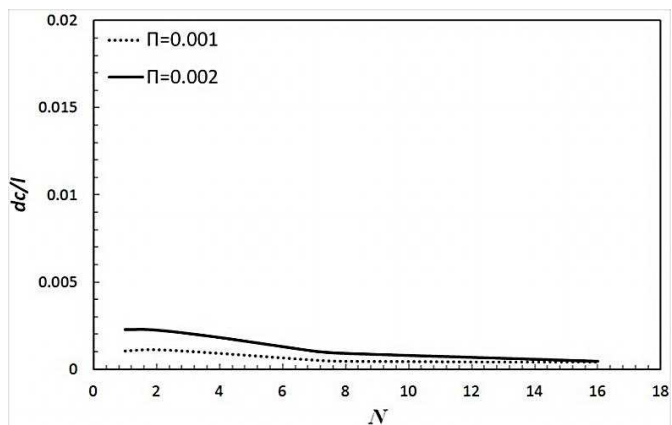


Fig. 18. Optimum normalized core member thickness with respect to the order of corrugation in the longitudinal loading

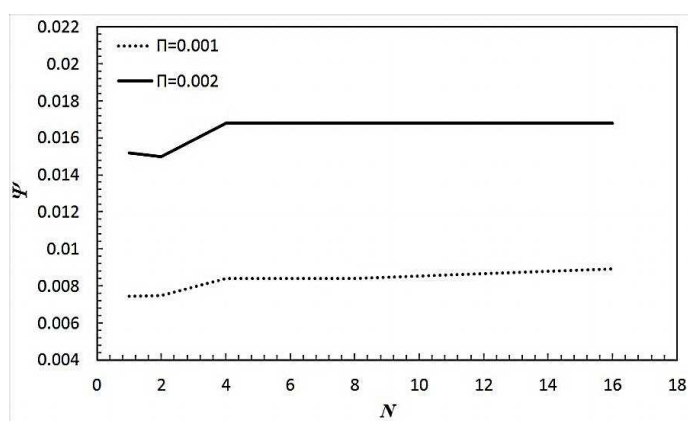


Fig. 19. Optimum weight index with respect to the order of corrugation in the longitudinal loading

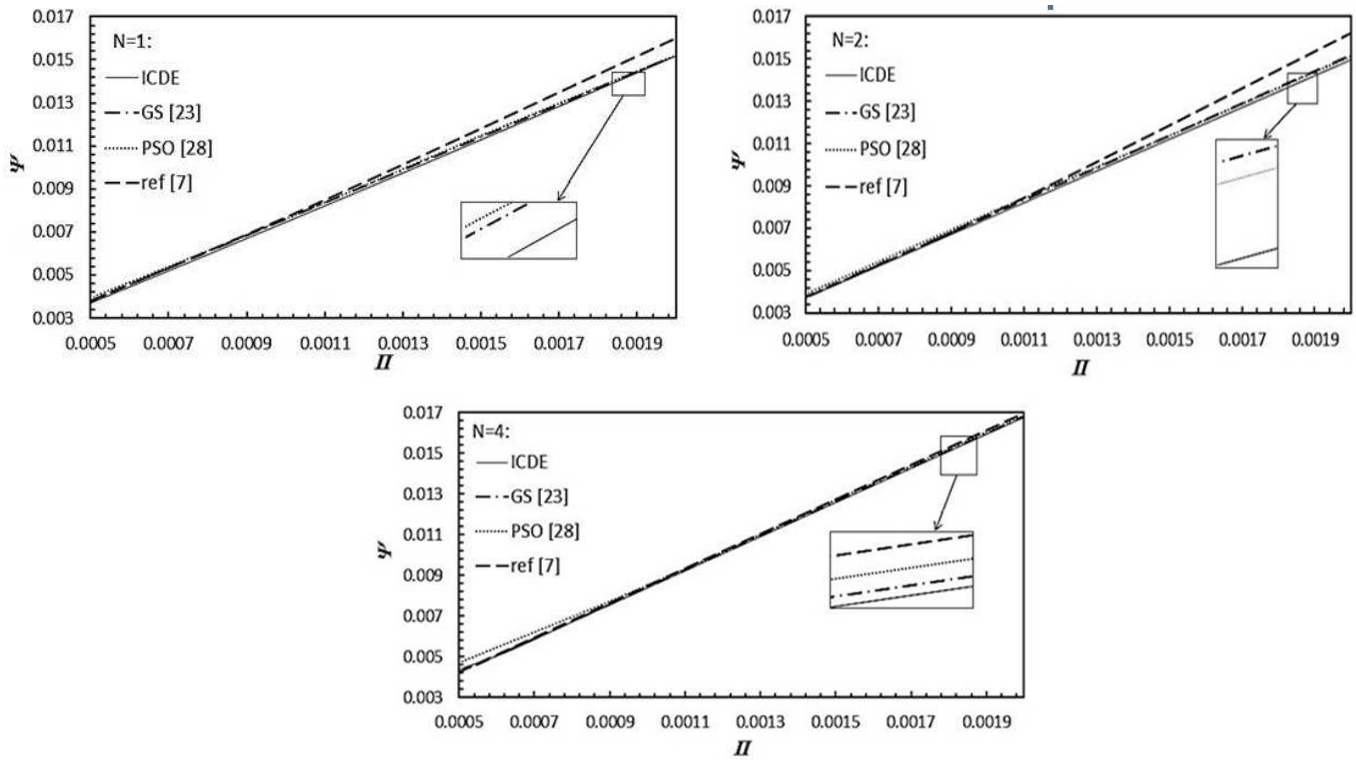


Fig. 20. Comparison of the optimum weight index obtained by ICDE algorithm with GS [35], PSO [40] and reference [10] in longitudinal loading for  $N=1,2,4$

### 6. Conclusion

In this research, the weight optimization of the prismatic core sandwich panel under different loading conditions has been proposed. The results of this study can be summarized as follows:

- For both types of loading, in order to prevent the yielding and buckling of the sandwich panel, values of the panel height, the face and core member thickness in addition to the weight index are increased by adding to the load index to avoid yielding and buckling of the panel.
- At a constant value of the load index, by increasing the core corrugate number, the weight index has a lowering behavior in the transverse loading and a rising behavior in the longitudinal loading. However, the face and core member thickness have a lowering behavior and the panel height has a rising behavior.
- According to the weight index value, panels with  $N=4$  and  $N=1$  are suitable respectively in the transverse and longitudinal loading for applications with size restrictions.
- The results in the transverse loading obtained in this study are equal to those of the previous works, but the results of the ICDE in the longitudinal loading are better.
- Another advantage of the ICDE is that there is no need for the time-consuming process of trial and error to fine-tuning the penalty function parameters. Thus it can be a robust alternative to the penalty function based methods for the sandwich panel optimization in the future works.

### Author Contributions

All authors discussed the results, reviewed and approved the final version of the manuscript.

### Conflict of Interest

The authors declared no potential conflicts of interest with respect to the research, authorship and publication of this article.

### Funding

The authors received no financial support for the research, authorship and publication of this article.

### Nomenclature

$d$  Face sheet thickness  
 $dc$  Core sheet thickness

**Greek symbols**  
 $\epsilon_y$  Yield strain



$CR, F$	Control parameters of ICDE	$\theta$	Angle between the folded core plate and the horizontal
$E$	Young's modulus	$\lambda$	Number of individuals in the parent population
$H$	Overall panel height	$\mu$	Number of individuals in the offspring population
$K_c$	Core buckling coefficient	$\vartheta$	Poisson ratio
$K_f$	Face buckling coefficient	$\Pi$	Load index
$N$	Order of corrugation	$\rho$	Density
$V$	Maximum shear load	$\sigma_y$	Yield stress
$\nu$	Mutation operator of ICDE	$\Psi$	Weight index
$W$	Weight of panel per unit width	<b>Subscripts</b>	
$x$	Solution vector in ICDE	$c$	Core
$y$	Distance from the center of the core member to the face member	$f$	face

## References

- [1] Zenkert, D., An Introduction to Sandwich Construction., *Engineering Materials Advisory Services*, 1995
- [2] Vinson, J.R. and R.L. Sierakowski, The Behavior of Structures Composed of Composite Materials, *The Netherlands: KLUWER Academic Publisher*, 2002.
- [3] Wang, Z., Recent advances in novel metallic honeycomb structure, *Composites Part B: Engineering*, 166, 2019, 731-741.
- [4] Wei, K., He, R., Cheng, X., Zhang, R., Pei, Y. and Fang, D., Fabrication and mechanical properties of lightweight ZrO<sub>2</sub> ceramic corrugated core sandwich panels, *Materials & Design*, 64, 2014, 91-95.
- [5] Wadley, H.N.G., N.A. Fleck, and A.G. Evans, Fabrication and structural performance of periodic cellular metal sandwich structures, *Composites Science and Technology*, 63(16), 2003, 2331-2343.
- [6] Zok, F.W., et al., A protocol for characterizing the structural performance of metallic sandwich panels: application to pyramidal truss cores, *International Journal of Solids and Structures*, 41(22-23), 2004, 6249-6271.
- [7] Lu, T.J., H.A. Stone, and M.F. Ashby, Heat transfer in open-cell metal foams, *Acta Materialia*, 46(10), 1998, 3619-3635.
- [8] Min, J.K., et al., High-temperature heat exchanger studies for applications to gas turbines, *Heat and Mass Transfer*, 46(2), 2009, 175-186.
- [9] Chen, W. and Hao, H., Experimental and numerical study of composite lightweight structural insulated panel with expanded polystyrene core against windborne debris impacts, *Materials & Design*, 60, 2014, 409-423.
- [10] Valdevit, L., J.W. Hutchinson, and A.G. Evans, Structurally Optimized Sandwich Panels with Prismatic Cores, *International Journal of Solids and Structure*, 41(18-19), 2004, 5105-5124.
- [11] Rathbun, H.J., F.W. Zok, and A.G. Evans, Strength optimization of metallic sandwich panels subject to bending, *International Journal of Solids and Structures*, 42(26), 2005, 6643-6661.
- [12] Liaghat, G. and H. Serailou, Core Optimal Design in Honeycomb Structures Under Compression Loading, *Modares Mechanical Engineering*, 9(37), 2009, 73-82.
- [13] Yan, L.L., Han, B., Yu, B., Chen, C.Q., Zhang, Q.C. and Lu, T.J., Three-point bending of sandwich beams with aluminum foam-filled corrugated cores, *Materials & Design*, 60, 2014, 510-519.
- [14] Rao, S.S., *Engineering Optimization: Theory and Practice*. 4th ed. 2009: John Wiley and Sons.
- [15] Bin, H., Bo, Y., Yu, X., Chang-Qing, C., Qian-Cheng, Z. and Jian, L.T., Foam filling radically enhances transverse shear response of corrugated sandwich plates, *Materials & Design*, 77, 2015, 132-141.
- [16] Dharmasena, K.P., Wadley, H.N., Xue, Z. and Hutchinson, J.W., Mechanical response of metallic honeycomb sandwich panel structures to high-intensity dynamic loading, *International Journal of Impact Engineering*, 35(9), 2008, 1063-1074.
- [17] Kabir, M.M., Wang, H., Lau, K.T., Cardona, F. and Aravinthan, T., Mechanical properties of chemically-treated hemp fiber reinforced sandwich composites, *Composites Part B: Engineering*, 43(2), 2012, 159-169.
- [18] Li, M., Wu, L., Ma, L., Wang, B. and Guan, Z., Mechanical response of all-composite pyramidal lattice truss core sandwich structures, *Journal of Materials Science & Technology*, 27(6), 2011, 570-576.
- [19] Yalkin, H.E., Icten, B.M. and Alpyildiz, T., Enhanced mechanical performance of foam core sandwich composites with through the thickness reinforced core, *Composites Part B: Engineering*, 79, 2015, 383-391.
- [20] Yu, B., Han, B., Su, P.B., Ni, C.Y., Zhang, Q.C. and Lu, T.J., Graded square honeycomb as sandwich core for enhanced mechanical performance, *Materials & Design*, 89, 2016, 642-652.
- [21] Wang, B., Hu, J., Li, Y., Yao, Y., Wang, S. and Ma, L., Mechanical properties and failure behavior of the sandwich structures with carbon fiber-reinforced X-type lattice truss core, *Composite Structures*, 185, 2018, 619-633.
- [22] Li, T. and Wang, L., Bending behavior of sandwich composite structures with tunable 3D-printed core materials, *Composite Structures*, 175, 2017, 46-57.
- [23] Prugel-Bennett, A., Benefits of a Population: Five Mechanisms That Advantage Population-Based Algorithms, *IEEE Transactions on Evolutionary Computation*, 14(4), 2010, 500-517.
- [24] Kennedy, R., 1995, November. J. and Eberhart, Particle swarm optimization, *In Proceedings of IEEE International Conference on Neural Networks*, 1000, 1995, 33.
- [25] Geem, Z., J. Kim, and G.V. Loganathan, A New Heuristic Optimization Algorithm: *Harmony Search*.

*SIMULATION*, 76(2), 2001,60-68.

[26] Yang, X.-S., A New Metaheuristic Bat-Inspired Algorithm, in Nature Inspired Cooperative Strategies for Optimization (NICSO 2010), J. González, et al., Editors., *Springer Berlin Heidelberg*, 2010, 65-74.

[27] Yang, X.S., Firefly algorithms for multimodal optimization, *In International Symposium on Stochastic Algorithms*, 2009, 169-178.

[28] Kaveh, A. and S. Talatahari, A novel heuristic optimization method: charged system search, *Acta Mechanica*, 213(3-4), 2010, 267-289.

[29] Eskandar, H., et al., Water cycle algorithm – A novel metaheuristic optimization method for solving constrained engineering optimization problems, *Computers & Structures*, 110–111, 2012, 151-166.

[30] Kaveh, A. and N. Farhoudi, A new optimization method: Dolphin echolocation, *Advances in Engineering Software*, 59, 2013, 53-70.

[31] Fereidoon, A., M. Mohammadian, and H. Hemmatian, Reliability-based optimization of a prismatic core sandwich panel, *Journal of Civil Engineering Optimization*, 22(1), 2011, 89-102.

[32] Banerjee, S., M. Battley, and D. Bhattacharyya, Shear Strength Optimization of Reinforced Honeycomb Core Materials, *Mechanics of Advanced Materials and Structures*, 17(7), 2010, 542-552.

[33] Hemmatian, H., A. Fereidoon, and M. Rajabpour, Optimization of prismatic core based on particle swarm algorithm, *Modeling in Engineering*, 8(20), 2010, 17-26.

[34] Fereidoon, A., et al., Sandwich Panel Optimization Based on Yielding and Buckling Criteria by Using of Imperialist Competitive Algorithm, *Modares Mechanical Engineering*, 13(4), 2013, 25-35.

[35] Mohammadian, M. and M.H. Abolbashari, investigation the Efficiency of Gravitational Search Algorithm in Optimization of Sandwich Structures under Longitudinal Loading with Yielding and Buckling Constraints, *Modares Mechanical Engineering*, 15(8), 2015,19-28.

[36] Tan, X.H. and A.K. Soh, Multi-objective optimization of the sandwich panels with prismatic cores using genetic algorithms, *International Journal of Solids and Structures*, 44(17), 2007, 5466-5480.

[37] Hudson, C.W., J.J. Carruthers, and A.M. Robinson, Multiple objective optimisation of composite sandwich structures for rail vehicle floor panels, *Composite Structures*, 92(9), 2010, 2077-2082.

[38] Khalkhali, A., S. Khakshournia, and N. Nariman-Zadeh, A Hybrid Method of FEM, Modified NSGAI and TOPSIS for Structural Optimization of Sandwich Panels with Corrugated Core, *Journal of Sandwich Structures and Materials*, 16(4), 2014, 398-417.

[39] Martínez-Martín, F.J. and A.P. Thrall, Honeycomb core sandwich panels for origami-inspired deployable shelters: Multi-objective optimization for a minimum weight and maximum energy efficiency, *Engineering Structures*, 69, 2014, 158-167.

[40] Mohammadian, M. and A. Fereidoon, Multi-Objective Optimization of Sandwich Panels Using Particle Swarm Algorithm, *Modares Mechanical Engineering*, 14(1), 2014, 74-82.

[41] Gu, S., T.J. Lu, and A.G. Evans, On the design of two-dimensional cellular metals for combined heat dissipation and structural load capacity, *International Journal of Heat and Mass Transfer*, 44(11), 2001, 2163-2175.

[42] Wang, Y., et al., Multiobjective Optimization and Hybrid Evolutionary Algorithm to Solve Constrained Optimization Problems, *IEEE Transactions on Systems, Man, and Cybernetics, Part B*, 37(3), 2007, 560-575.

[43] Coello Coello, C.A., Theoretical and numerical constraint-handling techniques used with evolutionary algorithms: a survey of the state of the art, *Computer Methods in Applied Mechanics and Engineering*, 191(11–12), 2002, 1245-1287.

[44] Jia, G., et al., An improved ( $\mu + \lambda$ ) constrained differential evolution for constrained optimization, *Information Sciences*, 222, 2013,302-322.

[45] Storn, R. and K. Price, Differential Evolution – A Simple and Efficient Heuristic for global Optimization over Continuous Spaces, *Journal of Global Optimization*, 11(4), 1997, 341-359.



© 2020 by the authors. Licensee SCU, Ahvaz, Iran. This article is an open-access article distributed under the terms and conditions of the Creative Commons Attribution-NonCommercial 4.0 International (CC BY-NC 4.0 license) (<http://creativecommons.org/licenses/by-nc/4.0/>).